Applied Energy Symposium 2019: Low carbon cities and urban energy systems
October 16-18, 2019, Xiamen, China
Paper ID: 0081

GEOMETRICAL EFFECT ON PERFORMANCE AND CATALYST VOLUME OF METHANE REFORMING WITH CO2 REACTORS FOR SOLAR THERMOCHEMICAL ENERGY STORAGE

Mingmin Kong [1], Chen Chen [1*]
1 Institute of Process Equipment and Control Engineering
Zhejiang University of Technology, Hangzhou,
Zhejiang, 310032
China

ABSTRACT

In CO_2 reforming of methane solar thermochemical energy storage, the endothermic methane reforming with CO_2 reaction is utilized to absorb solar energy. Although a lot of research has been done to enhance the thermochemical performance of the solar driven CO_2 reforming of methane reactor, there is little research conducted investigating the geometrical effect of reactor on the reactor thermochemical performance. Moreover, the catalyst cost is anticipated to be large. Minimizing the required catalyst volume is the key to reduce the capital cost of the CO_2 reforming of methane solar thermochemical energy storage system. But there is not much research investigating the geometrical effect on the catalyst volume. In this paper, a pseudo-homogeneous computational model is used to simulate methane reforming with CO_2 reaction in a tubular packed bed reactor. A parametric study is performed to investigate the geometrical effects of reactor on the reactor performance. The results show that methane conversion as well as outlet gas temperature increase with reactor diameter and/or reactor length increasing while the energy efficiency decreases with reactor diameter and/or reactor length increasing. There is a trade-off between increasing methane conversion and decreasing energy efficiency. As the required catalyst volume increases with reactor size increasing, there is a trade-off between increasing methane conversion and increasing catalyst volume. Another parametric study has been conducted to study the effects of reactor geometries on the required catalyst volume. The results show that the required catalyst volume can be saved by decreasing the reactor diameter due to enhanced heat transfer.

Keywords: Solar thermochemical energy storage, Methane reforming with carbon dioxide, Geometrical effect

NONMENCLATURE

Abbreviations	
TES	Thermal Energy Storage
STES	Sensible Thermal Energy Storage
LTES	Latent Thermal Energy Storage
TCES	Thermochemical Energy Storage
Symbols	
c_p	Specific heat of gas, J/(kg·K)
D_{eff}	Effective diffusivity, m^2/s
D_p	Hydraulic diameter, m
F	Equivalent particle diameter, m
E_a	Flow rate, L/min
ΔH	Activation energy, J/mol
$k_{o,m}$	Heat of reaction, J/kg
k	Pre-exponential constant, $kg/(m^3 \cdot s)$
K	Thermal conductivity, W/(m·K)
L	Equilibrium constant
P	Reactor length, m
q''_w	Pressure, Pa
$\dot{r}'''$	Heat flux, $W/(m^2 \cdot K)$
R_u	Rate of methanation, $kg/(m^3 \cdot s)$
T	Universal gas constant, J/(mol·K)
T_0	Temperature, °C

Selection and peer-review under responsibility of the scientific committee of CUE2019

U	Furnace operating temperature, °C
V_c	Heat transfer coefficient, W/(m^2·K)
v	Catalyst volume, m^3
X_{CH4}	Velocity, m/s
Y_{CH4}	X_{CH4} Methane conversion
ε	Y_{CH4} Methane volume fraction
η	Emissivity of the reactor wall
η_{en}	Effectiveness factor
μ	Energy efficiency
ρ	Viscosity of the gas mixture, Pa·s
	Density of the gas mixture, kg/m^3

1. INTRODUCTION

Solar energy is a renewable and widely-used alternative to the fossil fuel. In order to overcome the drawback of intermittence, thermal energy storage (TES) is used for solar power plants, e.g., using molten salt tanks, as a sensible thermal energy storage (STES), to store solar energy in solar power plants. Besides the STES, latent thermal energy storage (LTES) and thermochemical energy storage (TCES) are the common methods for TES [1]. Compared with the other two, thermochemical energy storage is superior with a higher energy density and the capability of storing energy in reactants at ambient temperature [2, 3]. The principle of a solar thermochemical energy storage system is to store and use solar energy with reversible reactions. Basically, solar energy is stored during the endothermic reaction, which is called as the charging step, and released during the exothermic reaction, which is called as the discharging step. A lot of scholars are currently studying many potential TCES systems with different reactions. But more breakthroughs are required to address the potential catalyst sintering caused by elevated operating temperature and insufficient heat transfer. Ammonia decomposition/synthesis TCES (ammonia-based TCES) is one of the most mature TCES [2, 3]. The charging loop, i.e., absorbing solar energy with ammonia decomposition, has been validated by Lovegrove and Kreetz et al. [4]. Moreover, the discharging loop, i.e., heating steam with ammonia synthesis, by Chen et al. [5-6]. However, there has not been a relatively cheap and safe method validated to store a large amount of the gaseous reactants, i.e., N_2 and H_2, which constrains the potential of incorporating the ammonia-based TCES with a commercial power plant. CO_2 reforming of methane, as thermochemical energy storage, has been investigated since 1990s [7]. On-sun tests of CO_2 reforming of methane have been conducted at Sun Yat-Sen University [8] with promising results. Compared with other TCES technologies, CO_2 reforming of methane is superior with a high energy density. Further, the excessive products of hydrogen can be used as a non-carbon fuel. Figure 1 shows a schematic of a CO_2 reforming of methane solar thermochemical energy storage system. As shown in Figure 1, methane (CH_4) and carbon dioxide (CO_2) from the storage tank react endothermically by absorbing solar energy. The products of hydrogen (H_2) and carbon monoxide (CO) flow back to the other storage tank. The stored energy can be released when the hydrogen (H_2) and carbon monoxide (CO) react exothermically to heat a working fluid for power cycles to generate electricity, e.g., supercritical carbon dioxide (sCO_2) for a Brayton cycle. A lot of research has been done on CO_2 reforming of methane solar thermochemical energy storage system, most of which focuses on the thermochemical performance of the reactor [8-10]. Recently, Lee et al. [11] studied the effect of the reactor radius on the hydrogen production of a membrane reactor for carbon dioxide reforming of carbon dioxide. However, the geometrical effect of reactor, i.e., reactor diameter and length, on the reactor thermochemical performance including energy efficiency, methane conversion and required catalyst volume are rarely investigated.

The CO_2 reforming of methane solar thermochemical energy storage system, shown in Figure 1, operates in a closed loop. Since there is no regularly recurring expense for feedstock, the cost of the system is mainly determined by the initial capital cost, including the costs of manufacturing material and the catalyst. Nickel-based catalyst is one of the most widely-used catalysts for CO_2 reforming of methane [12]. However, the cost of nickel-based catalyst is still expensive, which need be optimized for the system design. There has not been any investigation performed pertaining saving the catalyst cost of a solar driven methane reforming with CO_2 reactor. In this paper, a simulation model is presented for CO_2 reforming of methane reaction in a tubular packed bed. The model is also used to investigate the geometrical effect of reactor on the reactor performance, e.g., energy efficiency and methane conversion, and required catalyst volume.

2. MODELING

A pseudo-homogeneous model [6] is used to simulate the reaction kinetics and thermodynamics of reacting gas in a tubular packed bed. The model utilizes effective properties for fluid and solid phases. Figure 2 shows a schematic of a tubular packed reactor.

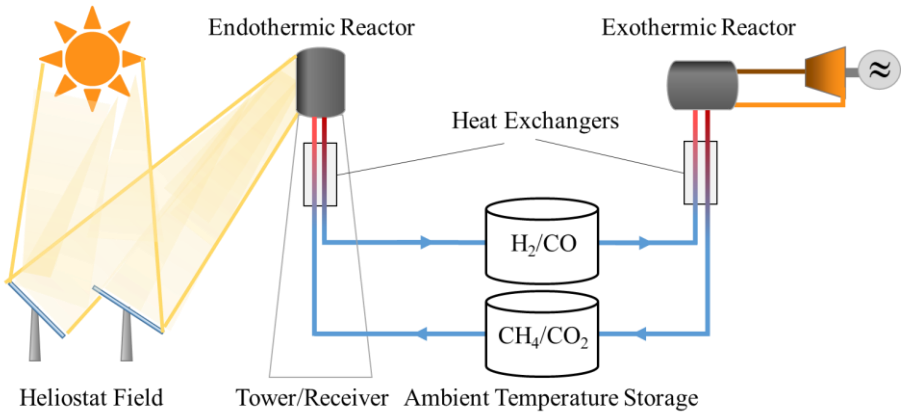

Fig 1 Schematic of a methane reforming thermochemical energy storage system.

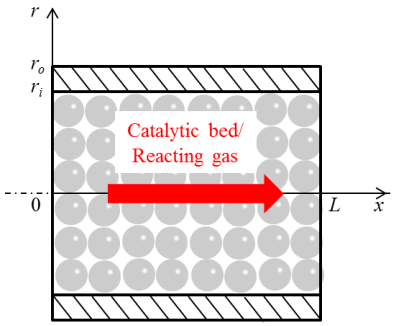

Fig 2 Schematic of a methane reforming with CO_2 reactor.

In this reactor, reacting gas is reacting endothermically (CO_2 reforming of methane reaction) in the catalyst bed. CO_2 reforming of methane consists of two reactions, i.e., the main reaction and the side reaction. The main reaction is the carbon dioxide reforming of methane (CRM):

$$\text{CRM: } CH_4 + CO_2 \rightleftarrows 2CO + 2H_2 \quad \Delta H^0_{298K} = 247 \text{ kJ/mol} \tag{1}$$

The side reaction is the reverse water gas shift (RWGS) processes:

$$\text{RWGS: } CO_2 + H_2 \rightleftarrows CO + H_2O \quad \Delta H^0_{298K} = 41 \text{ kJ/mol} \tag{2}$$

The energy conservation equation neglecting the axial conduction is:

$$\rho_g v_g c_{p,g} \frac{\partial T_g}{\partial x} = \frac{1}{r}\frac{\partial}{\partial r}\left(k_{eff} r \frac{\partial T_g}{\partial r}\right) + \dot{r}'''\Delta H \tag{3}$$

where ρ_g is the reacting gas density, v_g is the reacting gas velocity, $c_{p,g}$ is the reacting gas specific heat capacity, $\dot{r}'''$ is the reaction rate, ΔH is the heat of the reaction, and k_{eff} is the effective thermal conductivity. The boundary conditions for Eq. (3) are:

$$T_g(r, x=0) = T_{g,in} \tag{4}$$

$$k_{eff}\frac{\partial T_g}{\partial r}(r=r_1, x) = U_o\left[T_g(r=r_i, x) - T_w(x)\right] = q''_w \tag{5}$$

where U_o is the overall heat transfer coefficient at the catalyst bed outer wall, T_w is the wall temperature, and q''_w is the heat flux at the reactor wall. The overall heat transfer coefficient U_o accounts for the thermal conduction through the reactor wall. The heat flux at the reactor wall is determined by the radiation from a furnace outside of the reactor and heat loss to the ambient:

$$q''_w = \varepsilon\sigma\left(T_f^4 - T_w^4\right) + h_{loss}\left(T_a - T_w\right) \tag{6}$$

where T_f is the furnace radiant surface temperature, h_{loss} is the heat transfer coefficient for the heat loss, and T_a is the ambient temperature. Note that, $T_f = T_0 + 10$ K, where T_0 is the operating temperature for the furnace.

The mass conservation equation neglecting the axial diffusion is:

$$\rho_g v_g \frac{\partial X_{CH4}}{\partial x} = \rho_g D_{eff}\frac{1}{r}\frac{\partial}{\partial r}\left(r\frac{\partial X_{CH4}}{\partial r}\right) + \dot{r}''' \tag{7}$$

where X_{CH4} is the methane conversion. The corresponding boundary conditions for mass conservation are:

$$X_{CH4}(r, x=0) = X_{CH4,in} \tag{8}$$

$$\left.\frac{\partial X_{CH4}}{\partial r}\right|_{r_i} = 0 \tag{9}$$

In the model, the reaction rate $\dot{r}'''$ is determined by the kinetics of CRM reaction as RWGS reaction is assumed to be always at equilibrium. The chemical reaction kinetics is modeled based on the basic reaction model [13]:

$$\dot{r}''' = \eta k_{o,m}\exp\left(\frac{-E_a}{R_u T}\right)\left[P_{CH4}P_{CO2} - K_C^{-1}P_{CO}^2 P_{H2}^2\right] \tag{10}$$

where the effectiveness factor η accounts for the reactant concentration gradient within the catalyst particle. The equilibrium constant K_C based on the data from [14] is calculated as:

$$K_C = \exp(34.225 - 31299/T_g) \tag{11}$$

For the RWGS reaction (Equation 2), the chemical reaction kinetics is modeled as:

$$P_{CO2}P_{H2} = K_R^{-1}P_{CO}^2P_{H2O}^2 \quad (12)$$

where K_R is the equilibrium constant for the reaction, which is calculated based on the data from Callaghan [15].The reactor bed is filled with Ni/Al_2O_3 (Ni-15 wt%) catalyst with kinetic parameters listed in Table 1.

Table 1 The kinetic parameters for the model input

Activation energy, E_a (J/mol)	Pre-exponential constant, $k_{o,m}$ (kg/m^3·s)
5.8×10^3	1.36×10^9

The energy efficiency of the reactor η_{en} can be estimated as:

$$\eta_{en} = Q_r / \left(Q_r + Q_{loss}\right) \quad (13)$$

where Q_r is the rate at which energy is transferred to the reacting gas and Q_{loss} is the heat loss rate from the reactor.

3. RESULTS AND DISCUSSIONS

3.1 Model Validation

A FORTRAN code is developed to numerically solve the governing equations with a finite difference algorithm. The grids independency has been validated by setting the same model with more than twice of the grids. The results including the outlet gas temperature and conversion for the two different grids are similar with difference of 1%. In order to validate the model, the model generated methane conversions X_{CH4} for different furnace operating temperature T_0 are compared with experimental results from Lu et al. [10]. The properties and parameters used for model input including the inlet gas flow rate F_{in}, methane volume fraction Y_{CH4}, inlet gas temperature $T_{g,in}$, furnace operating temperature T_0, reactor length L, reactor inner diameter D_i, and reactor wall thickness W ($W=r_o-r_i$) are listed in Table 2.

Table 2 Properties of a sample case for the model

F_{in} (L/min)	Y_{CH4}	$T_{g,in}$ (°C)	T_0 (°C)	L (m)	D_i (cm)	W (cm)
4	0.5	550	800	0.2	2.6	0.2

Figure 3 shows the comparison of model generated methane conversion $X_{CH4,m}$ and experimental measured one $X_{CH4,exp}$ from literature [10]. As shown in Figure 3, the model generated results are in good agreement with the experimental results with the maximum deviation of 11% at T_0=750 °C. Based on the validation of the model, parametric studies were performed to investigate the effect of reactor geometries, i.e., reactor inner diameter D_i and reactor length L, on the performance of the reactor, i.e., energy efficiency η and methane conversion X_{CH4}. Moreover, the effect of reactor geometries on the required catalyst volume is explored as well.

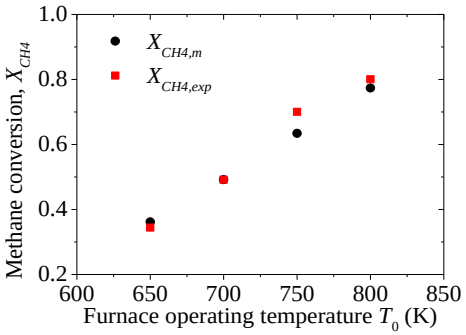

Fig 3 Comparison of model generated methane conversion $X_{CH4,m}$ and experimental measured one $X_{CH4,exp}$ [10].

3.2 Geometrical Effect on Reactor Performance

3.2.1 Effect of Diameter

For the solar driven CO_2 reforming of methane reactor, the performance is expected to be affected by the reactor diameter since both residence time and heat transfer depends on the reactor diameter. A parametric investigation is performed to study the effect of reactor inner diameter D_i (see Figure 2) on the reactor performance. In this investigation, the inner diameter D_i is varied from 1.5 to 3.5 cm while the reactor length is fixed to be 0.4 m. Other fixed conditions i.e., the inlet gas flow rate F_{in}, the CH_4 volume fraction Y_{CH4}, the gas inlet temperature $T_{g,in}$, the furnace operating temperature T_0, the reactor length L and the reactor wall thickness W, are fixed and listed in Table 2. Figure 4 shows methane conversion X_{CH4} and outlet gas temperature $T_{g,out}$ for different reactor inner diameters D_i. As shown in Figure 4, both methane conversion X_{CH4} and outlet gas temperature $T_{g,out}$ increase with reactor diameter D_i increasing. That is because the residence time increases with reactor diameter D_i increasing. As $T_{g,out}$ approaches to a high temperature ~790 °C, the increasing rates of both X_{CH4} and $T_{g,out}$ become quite moderate. That is because the heat loss, affected by the temperature difference between the reactor and the ambient, increases with reactor temperature increasing. Meanwhile the radiation from the furnace, determined by the temperature difference between the reactor and the furnace, decreases with reactor temperature increasing. Figure 5 shows the heat loss Q_{loss} and energy efficiency η_{en} of the reactor for different reactor inner diameters D_i. As expected, the heat loss Q_{loss} (in Figure 5) increases with D_i increasing because of increasing surface area. Although heat transferred to the reacting

gas Q_r also increases with inner diameter D_i increasing, the energy efficiency η_{en} (in Figure 5) decreases with D_i increasing. Therefore, there is a trade-off between increasing X_{CH4} and decreasing η_{en} when D_i is varied.

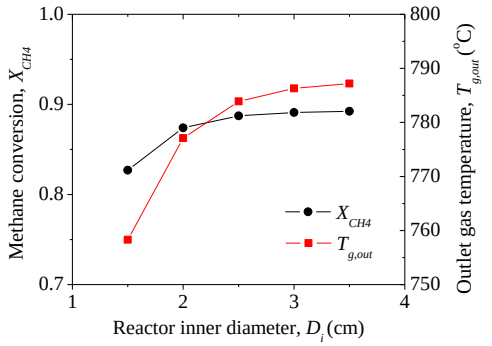

Fig 4 Methane conversion X_{CH4} and outlet gas temperature $T_{g,out}$ as functions of inner diameter D_i.

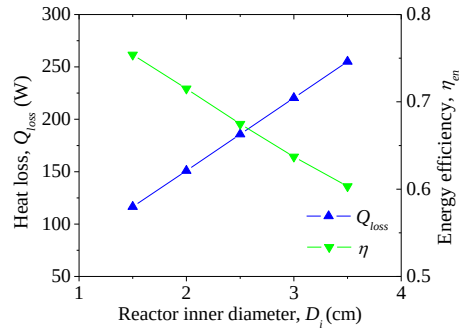

Fig 5 Heat loss Q_{loss} and energy efficiency η_{en} of the reactor as functions of reactor inner diameter D_i.

3.2.2 Effect of Length

The reactor length L is also a crucial factor affecting the reactor performance since the residence time depends on the reactor length L. A parametric investigation is performed to study the effect of the length L on the reactor performance. In this investigation, the reactor length L is varied from 10 to 50 cm while the diameter D_i is fixed to be 2.5 cm. Other fixed conditions listed in Table 2. Figure 6 shows methane conversion X_{CH4} and outlet gas temperature $T_{g,out}$ for different reactor length L. Similar to the case of increasing D_i (in Figure 6), both X_{CH4} and $T_{g,out}$, shown in Figure 6, increase with L increasing due to longer residence time. Figure 7 shows the heat loss Q_{loss} and energy efficiency η_{en} of the reactor for different reactor length L. As shown in Figure 7, Q_{loss} increases with L increasing while η_{en} decreases with L increasing because of heat loss surface area increasing. There is a trade-off between increasing X_{CH4} and decreasing η_{en} when L is varied.

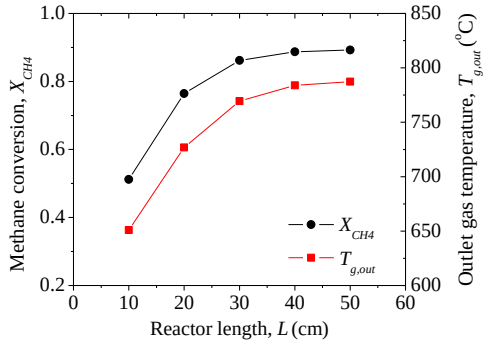

Fig 6 Methane conversion X_{CH4} and outlet gas temperature $T_{g,out}$ as functions of reactor length L.

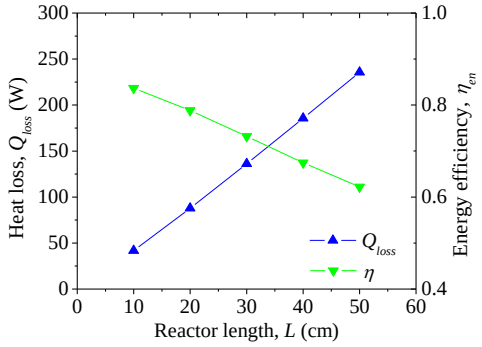

Fig 7 Heat loss Q_{loss} and energy efficiency η_{en} as functions of reactor length L.

3.3 Geometrical Effect on Required Catalyst Volume

Based on the previous discussion, the methane conversion and the outlet gas temperature can be increased by increasing reactor diameter and/or reactor length, which increases the required catalyst volume as well. In this section, the effect of geometries on the required catalyst volume is investigated by varying both reactor inner diameter D_i and reactor length L simultaneously while both the methane conversion X_{CH4} and outlet gas temperature $T_{g,out}$ are fixed. Table 3 lists all the fixed conditions. Figure 8 shows the reactor length L and required catalyst volume V_c for different reactor inner diameter D_i. As shown in Figure 8, L increases with D_i decreasing. But V_c decreases with D_i decreasing. That is because the heat transfer is enhanced by decreasing D_i. Thus, smaller reactor diameter is preferred in saving catalyst cost to achieve a fixed methane conversion X_{CH4}.

Table 3 Fixed conditions for studying the effect of geometries on required catalyst volume

F_{in} (L/min)	Y_{CH4}	$T_{g,in}$ (°C)	T_0 (°C)	W (cm)	X_{CH4}	$T_{g,out}$ (°C)
4	0.5	550	800	0.2	0.89	784

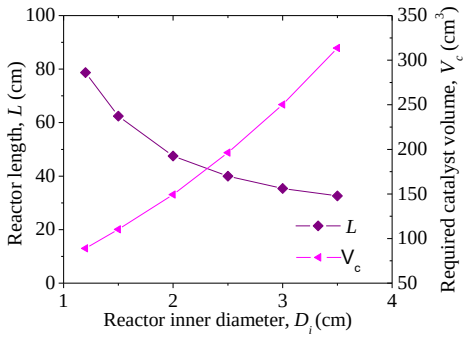

Fig 8 Reactor length L and required catalyst volume V_c as functions of reactor diameter D_i.

4. CONCLUSIONS

This paper has investigated performance and required catalyst volume of a solar driven methane reforming with CO_2 reactor. A pseudo-homogeneous model has been used to simulate CO_2 reforming of methane reaction in a tubular packed bed reactor. A parametric study was conducted to investigate the geometrical effects on the reactor performance, i.e., methane conversion and energy efficiency. The results show that both methane conversion and outlet gas temperature increase with reactor diameter and/or reactor length increasing while the energy efficiency decreases with reactor diameter and/or reactor length increasing. There is a trade-off between increasing the methane conversion and decreasing the energy efficiency. Similarly, there is a trade-off between increasing the methane conversion and increasing the required catalyst volume since the required catalyst volume increase with reactor diameter and/or reactor length increasing. Another parametric study is needed to investigate the effect of geometries on the desired catalyst volume when methane conversion is fixed. The results show that the required catalyst volume can be saved by decreasing the reactor diameter due to enhanced heat transfer. The analysis presented here provides a baseline for further design refinement and economic analysis.

REFERENCE

[1] Pelay U, Lu LA, Fan YL, Stitou D, Rood M. Thermal energy storage systems for concentrated solar power plants. Renew Sust Energ Rev. 2017;79:82-100.

[2] Pardo P, Deydier A, Anxionnaz-Minyielle Z, Rouge S, Cabassud M, Cognet P. A review on high temperature thermochemical heat energy storage. Renew Sust Energ Rev. 2014;32:591-610.

[3] Chen X, Zhang Z, Qi C, Ling X, Peng H. State of the art on the high-temperature thermochemical energy storage systems. Energ Convers Manage. 2018;177:792-815.

[4] Kreetz H, Lovegrove K. Exergy analysis of an ammonia synthesis reactor in a solar thermochemical power system. Solar Energy. 2002;73:187-94.

[5] Chen C, Zhao L, Kong M, Lavine AS. Heat recovery from an autothermal ammonia synthesis reactor for solar thermochemical energy storage. Solar Energy. 2018;176:256-66.

[6] Chen C, Aryafar H, Lovegrove KM, Lavine AS. Modeling of ammonia synthesis to produce supercritical steam for solar thermochemical energy storage. Solar Energy. 2017;155:363-71.

[7] Edwards JH, Maitra AM. The Chemistry of Methane Reforming with Carbon-Dioxide and Its Current and Potential Applications. Fuel Process Technol. 1995;42:269-89.

[8] Yu T, Yuan QY, Lu JF, Ding J, Lu YL. Thermochemical storage performances of methane reforming with carbon dioxide in tubular and semi-cavity reactors heated by a solar dish system. Appl Energ. 2017;185:1994-2004.

[9] Yuan QY, Ding J, Lu JF, Yu T, Wang WL. Heat transfer and energy storage performance of methane reforming with carbon dioxide in semi-cavity reactor. Selected Papers from Ix International Conference on Computational Heat and Mass Transfer (Icchmt2016). 2016;157:365-73.

[10] Lu JF, Chen Y, Ding J, Wang WL. High temperature energy storage performances of methane reforming with carbon dioxide in a tubular packed reactor. Appl Energ. 2016;162:1473-82.

[11] Lee B, Yun S-W, Kim S, Heo J, Kim Y-T, Lee S, et al. CO2 reforming of methane for H2 production in a membrane reactor as CO2 utilization: Computational fluid dynamics studies with a reactor geometry. Int J Hydrogen Energ. 2019;44:2298-311.

[12] Nandini A, Pant KK, Dhingra SC. Kinetic study of the catalytic carbon dioxide reforming of methane to synthesis gas over Ni-K/CeO2-Al2O3 catalyst. Applied Catalysis a-General. 2006;308:119-27.

[13] Mark MF, Mark F, Maier WF. Reaction kinetics of the CO2 reforming of methane. Chemical Engineering & Technology. 1997;20:361-70.

[14] Yaw TC, Saidina A. ANALYSIS OF CARBON DIOXIDE REFORMING OF METHANE VIA THERMODYNAMIC EQUILIBRIUM APPROACH. Jurnal Teknologi. 2005;43:161–7.

[15] Callaghan CA. Kinetics and Catalysis of the Water-Gas-Shift Reaction: A Microkinetic and Graph Theoretic Approach. 2006.